Acta Pharmaceutica Sinica B 2024;14(2):667−681

Chinese Pharmaceutical Association
Institute of Materia Medica, Chinese Academy of Medical Sciences

Acta Pharmaceutica Sinica B

www.elsevier.com/locate/apsb
www.sciencedirect.com

ORIGINAL ARTICLE

Targeting cAMP in D1-MSNs in the nucleus accumbens, a new rapid antidepressant strategy

Yue Zhang[a], Jingwen Gao[a], Na Li[a], Peng Xu[b], Shimeng Qu[a], Jinqian Cheng[a], Mingrui Wang[c], Xueru Li[d], Yaheng Song[a], Fan Xiao[a], Xinyu Yang[e], Jihong Liu[e], Hao Hong[f], Ronghao Mu[f], Xiaotian Li[g], Youmei Wang[b], Hui Xu[a], Yuan Xie[a], Tianming Gao[e], Guangji Wang[a,*], Jiye Aa[a,*]

[a]*Jiangsu Provincial Key Laboratory of Drug Metabolism and Pharmacokinetics, State Key Laboratory of Natural Medicines, Research Unit of PK−PD Based Bioactive Components and Pharmacodynamic Target Discovery of Natural Medicine of Chinese Academy of Medical Sciences, China Pharmaceutical University, Nanjing 210009, China*
[b]*Key Laboratory of Drug Monitoring and Control, Drug Intelligence and Forensic Center, Ministry of Public Security, Beijing 100193, China*
[c]*School of Pharmacy, China Pharmaceutical University, Nanjing 211198, China*
[d]*School of Foreign Languages, China Pharmaceutical University, Nanjing 211198, China*
[e]*Department of Neurobiology, School of Basic Medical Sciences, Southern Medical University, Guangzhou 510515, China*
[f]*Department of Pharmacology, China Pharmaceutical University, Nanjing 211198, China*
[g]*School of Pharmaceutical Sciences, Zhengzhou University, Zhengzhou 450001, China*

Received 13 June 2023; received in revised form 11 September 2023; accepted 14 November 2023

KEY WORDS

cAMP;
Nucleus accumbens;
Depression;
D1-MSN;
D2-MSN;

Abstract Studies have suggested that the nucleus accumbens (NAc) is implicated in the pathophysiology of major depression; however, the regulatory strategy that targets the NAc to achieve an exclusive and outstanding anti-depression benefit has not been elucidated. Here, we identified a specific reduction of cyclic adenosine monophosphate (cAMP) in the subset of dopamine D1 receptor medium spiny neurons (D1-MSNs) in the NAc that promoted stress susceptibility, while the stimulation of cAMP production in NAc D1-MSNs efficiently rescued depression-like behaviors. Ketamine treatment enhanced

*Corresponding authors.
E-mail addresses: guangjiwang@hotmail.com (Guangji Wang), jiyea@cpu.edu.cn (Jiye Aa).
Peer review under the responsibility of Chinese Pharmaceutical Association and Institute of Materia Medica, Chinese Academy of Medical Sciences.

https://doi.org/10.1016/j.apsb.2023.12.005
2211-3835 © 2024 The Authors. Published by Elsevier B.V. on behalf of Chinese Pharmaceutical Association and Institute of Materia Medica, Chinese Academy of Medical Sciences. This is an open access article under the CC BY-NC-ND license (http://creativecommons.org/licenses/by-nc-nd/4.0/).

Rapid antidepressant;
Crocin;
Ketamine

cAMP both in D1-MSNs and dopamine D2 receptor medium spiny neurons (D2-MSNs) of depressed mice, however, the rapid antidepressant effect of ketamine solely depended on elevating cAMP in NAc D1-MSNs. We discovered that a higher dose of crocin markedly increased cAMP in the NAc and consistently relieved depression 24 h after oral administration, but not a lower dose. The fast onset property of crocin was verified through multicenter studies. Moreover, crocin specifically targeted at D1-MSN cAMP signaling in the NAc to relieve depression and had no effect on D2-MSN. These findings characterize a new strategy to achieve an exclusive and outstanding anti-depression benefit by elevating cAMP in D1-MSNs in the NAc, and provide a potential rapid antidepressant drug candidate, crocin.

© 2024 The Authors. Published by Elsevier B.V. on behalf of Chinese Pharmaceutical Association and Institute of Materia Medica, Chinese Academy of Medical Sciences. This is an open access article under the CC BY-NC-ND license (http://creativecommons.org/licenses/by-nc-nd/4.0/).

1. Introduction

The growing prevalence of major depressive disorder (MDD) and the shortcomings in the effectiveness of currently available antidepressants cause substantial health and socioeconomic burdens, highlighting the need for new, rapid, and improved treatments[1,2]. Several factors, such as genetic variations, environmental factors, and inflammation, are considered to be important determinants of both susceptibility and resilience to MDD[3–7]. However, thus far, the pathogenesis of MDD is still inconclusive.

Preclinical and clinical evidence suggests that dysfunctions in the brain's reward system contribute to depressed mood, reduced motivation, and anhedonia, which are prominent symptoms of major depression[8–12]. Reciprocally, functional improvements in the reward circuit are relevant to reduced symptoms of hopelessness and anhedonia by antidepressant treatment[13,14]. The nucleus accumbens (NAc) is a crucial region within the brain's reward circuit and has been implicated in reward processing, as well as the pathophysiology of major depression[14–17]. The NAc hosts primarily medium spiny neurons (MSNs), but the functions of these MSNs are quite heterogeneous. The different subsets of MSNs (including dopamine receptor 1, D1R, and dopamine receptor 2, D2R), as well as MSNs in different NAc subdivisions, may antagonize each other and operate in opposite ways[18–21]. Therefore, the regulatory strategy that targets the NAc to achieve an exclusive and outstanding antidepressant benefit has not been elucidated, nor have antidepressants based on this strategy been developed to benefit patients with MDD.

Recent studies suggest that neuronal cyclic adenosine monophosphate (cAMP) in the NAc orchestrates stress vulnerability[17,22]; however, the specific groups of neurons in the NAc that involved in cAMP-mediated stress vulnerability remain elusive. Here, we identified that a specific reduction of cAMP in the subset of D1-MSNs in the NAc promotes stress susceptibility and that the stimulation of cAMP production in NAc D1-MSNs rescues depressive behaviors. cAMP is a second messenger involved in controlling adaptive cellular responses, and the efficacy of antidepressant pharmacotherapy ultimately points to the homeostatic regulation of intracellular cAMP, thereby impacting the effects of stress and depression-like behaviors[22–27]. Tellingly, we discovered that crocin is of great potential to rapidly relieve depression by regulating D1-MSN cAMP signaling in the NAc.

2. Materials and methods

2.1. Animals

All animal care and experimental procedures were approved by the Animal Ethics Committee of China Pharmaceutical University and performed in accordance with the U.S. National Institutes of Health Guidelines. Male C57BL/6J mice (7−8 weeks) and male breeding-retired CD-1 mice (6−7 months) were obtained from Vital River Laboratories (Beijing, China). *Drd1a*-Cre (D1-Cre) mice (RRID: MMRRC#034259-UCD) and *Drd2*-Cre (D2-Cre) mice (RRID: MMRRC#017268-UCD) were obtained from the MMRRC. Rosa26-LSL-tdTomato mice, D1-tdTomato and D2-tdTomato were obtained from Shanghai Biomodel Organism Center, Inc. Mice were genotyped using PCR and confirmed by sequencing. PCR primers for D1-Cre mice were as follows: *Drd1a* F1: GCTATGGAGATGCTCCTGATGGAA; *CreGS* R1: CGGCAAACGGACAGAAGCATT. PCR primers for D2-Cre mice are: *Drd2* (17268) F1: GTGCGTCAGCATTTGGAGCAA; *CreGS* R1: CGGCAAACGGACAGAAGCATT. PCR primers for tdTomato mice are as follows: *tdTomato* mutant-F: GGCATTAAAGCAGCGTATCC; *tdTomato* mutant-R: CTGTTCCTGTACGGCATGG; and *wild-type*-F: AAGGGAGCTGCAGTGGAGTA; *wild-type*-R: CCGAAAATCTGTGGGAAGTC. C57BL/6J mice, 5 per cage, and CD-1 mice, singly, were housed in a 12-h-light/12-h-darkness environment (temperature, 24 ± 1 °C; humidity, 45 ± 5 %), with standard mouse chow and water provided *ad libitum*. The mice were acclimated for a minimum of 7 days and then randomly assigned to different experimental groups.

2.2. Depression paradigms

2.2.1. Chronic unpredictable mild stress (CUMS)

Mice were habituated to 1% sucrose solution, and sucrose preference was tested weekly as the baseline. The mice were randomly grouped following the second test, according to their sucrose preference scores. Then the mice were subjected to a variety of mild stressors, including forced swimming in ice-cold water (10 min), restraint (4 h), wet bedding (12 h), food and water deprivation (24 h), social defeat (10 min), tail suspension (30 min), and night lighting (12 h). Two stressors were randomly assigned each day and this schedule lasted for 10 weeks[28].

2.2.2. Chronic social defeat stress (CSDS)

CSDS was performed according the protocol[29]. Male breeding-retired CD-1 mice were screened according to their appropriate aggressive behaviors. A plastic divider, contained holes, was placed in the middle of the cage, and the CD-1 aggressor mouse and C57BL/6J mouse were physically separated following defeat sessions. The C57BL/6J mouse was exposed to a novel CD-1 aggressor mouse for 10 min each day for a total of 10 days. The C57BL/6J mice were monitored for wounds and due care was made to avoid infection. The control mice were housed in pairs without stress. Depression or not was assessed using social interaction test, which was performed 24 h after the last defeat.

2.2.3. Chronic restraint stress (CRS)

50-mL conical tubes with holes were used for restraint stress. C57BL/6J mice were placed in the tubes for 4−6 h per day for 21 consecutive days. The tubes were thoroughly cleaned and disinfected with an odorless cleaning solution, and wiped dry every day[30].

2.3. Behavioral assays

2.3.1. Social interaction test

Social interaction (SI) test was performed in an open-field arena (40 cm × 40 cm × 40 cm), with a small wire cage placed on one side, which is large enough to clearly display a target CD-1 mouse. The test arena around the wire cage is defined as "interaction zone". Two 150-s phases were recorded with a Logitech camera. During the first phase, C57BL/6J mouse was placed into the open field opposite the empty wire cage. While the same metrics were measured in the second phase, but with a novel CD-1 aggressor in the wire cage. The SI ratio, obtained by dividing the time spent in the interaction zone when the target is present by the target is absent, less than 1 was grouped as susceptible, otherwise grouped as resilient[29].

2.3.2. Tail suspension test

Tail suspension test (TST) was performed in the tail suspension box, and mice were blinded to each other. Mice were individually suspended by tail with medical proof fabric, about 20 cm above the ground. The test lasted for 6 min, and the immobility time was counted during the last 4 min by two observers blinded to the animal treatment[31].

2.3.3. Forced swim test

Forced swim test (FST) was measured in glass beakers placed in the tail suspension box, making the mice blind to each other. Mice were individually placed in a 5-L glass beaker (height 27.5 cm, diameter 17.8 cm), containing 18−20 cm of water (24 ± 1 °C). Swimming behavior was videotaped for 6 min and the immobility time was measured during the final 4 min by two colleagues blinded to the study conditions[32].

2.3.4. Sucrose preference test

Mice were singly housed and habituated to water and 1% sucrose for 24 h, then deprived of food and drink for 12 h. The sucrose preference test (SPT) was performed during the dark period for 12 h, while mice were individually housed with free access to water and 1% sucrose. The bottles were weighed at the beginning and the end of the test. The preference was calculated by dividing the amount of sucrose consumed by the total amount of both water and sucrose consumed[33].

2.3.5. Coat score assay

The coat state is a reliable metric of depression in a mouse model[34,35]. Seven different body parts were measured, including head, neck, dorsum, ventrum, tail, forepaws and hind paws. A score of 1 was given to each of these areas if it was well groomed, and a score of 0 was given to each of these areas if it was unkempt. Total coat score was assayed as the sum of the seven areas.

2.3.6. Open field test

Mice were individually placed in an open-field arena (40 cm × 40 cm × 40 cm). The movement of each mouse was videotaped for 6 min, the time spent in the central zone was measured using Any-maze software.

2.3.7. Nesting behavior test

Mice were individually housed and habituated for 48 h. Two hours before nocturnal rhythm, 16 unscented napkins (4.5 cm × 4.5 cm) were spread on the bedding. The test lasted for 18 h, and the nesting was evaluated according to a 4-point method: 1, equates to the napkins scattered all over the cage without being bitten; 2, equates to the napkins gathered to one side of the cage, but loose, without shaped nest; 3, equates to the napkins gathered and folded into a shaped but flat nest, without obvious biting; 4, equates to the napkins gathered and folded into a deeper nest and bitten to small pieces. All mice were scored by observers blinded to animal treatment[36].

2.3.8. Marble burying test

The mice were singly housed with 5 cm deep sawdust bedding, depriving of food and water. At the beginning of the test, 16 glass beads (diameter 1.5 cm) were placed evenly on the bedding. The amount of buried beads was calculated 30 min later, and at least two-thirds of them were buried would be regarded as compulsive behavior[37].

2.3.9. Rotating-stick test

The motor coordination ability was evaluated on the rotarod system. The mice were pre-adapted to the rotarod apparatus at a speed of 20 rpm for 2 days. At the third day, the mice were placed on the apparatus one by one, and latency time to fall from the rotating stick was recorded for each animal[38].

2.3.10. Morris water maze

Spatial learning and memory were evaluated by the Morris water maze. The system consists of a steel tub (diameter 100 cm, height 38 cm), an adjustable stand (diameter 6 cm, height 14 cm) used for escaping, and an image collection and analysis system. The water temperature was set to 24 °C. The mice were skilled to find the platform for 6 days. On the 7th day, the platform was removed, the mice were placed in the tub and the numbers of passing through the platform area for a duration of 90 s were recorded. Tests were performed in dark condition and at the same time every day.

2.4. Animal treatments

Crocin (molecular weight: 976.97, purity: 98.04%) was purchased from Chengdu Biopurify Phytochemicals Ltd. (Chengdu, China). Citalopram (purity: 98%) was purchased from Aladdin (Shanghai). Ketamine was provided by the Drug Monitoring and Control Center, Ministry of Public Security. To examine the antidepressant effect of crocin, low-dose of 100 mg/kg, high-dose

of 300 mg/kg crocin (i.g.) and 20 mg/kg citalopram (positive control, i.p.) were given after the success of the depression model, once daily and lasted for 6 weeks[39,40]. To examine the rapid antidepressant effect of crocin, a single administration of ketamine (10 mg/kg, i.p.) was used as the positive control. Following the 10-day CSDS protocol, susceptible mice were given 100 mg/kg or 300 mg/kg crocin (i.g.). Following the 21-day CRS protocol, the mice were randomly grouped and given 100 or 300 mg/kg crocin (i.g.) or vehicle control. For intragastric administration, all drugs were ground using 0.5% CMC-Na. For intraperitoneal administration, drugs were dissolved in 0.9% saline. To test the safety of high-dose crocin (300 mg/kg), vehicle control or 300 mg/kg crocin were administered by gavage once daily for 7 days. Then the liver and kidney damage were detected, as well as the behavioral tests.

2.5. *Implantation of the microinjection cannula and drug treatments*

Mice were anesthetized with isoflurane and mounted in the small-animal stereotaxic frame (RWD Life Science). The cannula system (double cannula, 26G) was placed into the brain and leveled to the upper part of bilateral NAc (anteroposterior +1.6 mm, mediolateral ±1.3 mm, and dorsoventral −4.5 mm, according to the bregma), and fixed on the skull with dental cement[41]. Post-surgically mice were allowed to recover for one week. The agonists and antagonists of D1R and D2R (SKF81297C, SCH23390, quinpirole and Eticlopride, 1 μg/0.5 μL/side) were microinjected and behavioral tests were conducted 1 h later[42,43].

2.6. *Immunofluorescence*

Mice were transcardially perfused with saline and followed by 4% paraformaldehyde. Brains were removed and postfixed in 4% paraformaldehyde overnight at 4 °C. Then the brains were dehydrated in succession using 15% and 30% sucrose. After sinking to the bottom, the brains were embedded by OCT and immediately stored at −80 °C. The blocks were rewarmed at −20 °C more than 30 min prior to being sliced into 15 μm sections (Leica, CM1950). After washing with 0.1 mol/L PBS, the slices were blocked with 5% BSA for 2 h at room temperature and overnight incubated with primary antibodies at 4 °C, using mouse anti-cAMP (1:100, Santa Cruz, sc-73761). After three washes with PBS, slices were incubated with secondary antibodies for 2 h at room temperature away from light, using anti-mouse-Cy5 (1:200, Jackson Immunoresearch, #715-175-150). The sections were washed again with PBS and incubated with DAPI for 10 min, washed and mounted on ProLong Diamond Antifade Mountant (Invitrogen). The immunofluorescence images were acquired using FV3000 (Olympus). The tdTomato was auto-fluoresced with E_x: 561 nm and E_m: 590 nm; EGFP was auto-fluoresced with E_x: 488 nm and E_m: 509 nm.

2.7. *Fluorescence in situ hybridization (FISH)*

For D1-tdTomato and D2-tdTomato mice, the fixed brain blocks were prepared as previously described[44]. 10 μm coronal sections were prepared using freezing microtome, then stained with an RNAscope multiplex fluorescent reagent kit that provided by ACD Bio, the probes were designed by ACD Bio. The processing procedure was performed according to the manufacturer's standard protocols. The fluorescence images were acquired using FV3000 (Olympus).

2.8. *Ex vivo electrophysiology*

D1-tdTomato or D2-tdTomato mice were anesthetized with isoflurane and transcardially perfused with cold cutting solution saturated with 95% O_2 and 5% CO_2. The brain was quickly frozen in the cold cutting solution for 1 min. Then the brain was sliced into 300 μm coronal brain slices using oscillating blade microtome (Vibroslicer) in a cold oxygenated cutting solution containing: 4.5 mmol/L KCl, 40 mmol/L NaCl, 1.25 mmol/L $NaH_2PO_4 \cdot 2H_2O$, 25 mmol/L $NaHCO_3$, 148.5 mmol/L sucrose, 10 mmol/L dextrose$\cdot H_2O$, 1 mmol/L ascorbate, 3 mmol/L sodium pyruvate, 3 mmol/L inositol, 7 mmol/L $MgSO_4$, and 0.5 mmol/L $CaCl_2$ (pH 7.4). The brain slices containing nucleus accumbens were removed and incubated at 34 °C for 40 min in the oxygenated recording solution containing: 125 mmol/L NaCl, 4.5 mmol/L KCl, 1.25 mmol/L $NaH_2PO_4 \cdot 2H_2O$, 25 mmol/L $NaHCO_3$, 15 mmol/L sucrose, 15 mmol/L dextrose$\cdot H_2O$, 1.3 mmol/L $MgSO_4$, and 2.5 mmol/L $CaCl_2$ (pH 7.4).

The whole-cell current clamp recordings were obtained using MultiClamp700B (Molecular Devices, Axon). Briefly, the nucleus accumbens containing slice was placed and fixed in the fusionson chamber, and MSNs in the nucleus accumbens were visually identified by tdTomato-positive or tdTomato-negative (Olympus BX51WI, Irred CCD system). After the glass electrode was placed on the MSNs soma, a negative pressure was applied to form a seal. When the seal resistance exceeded 1 GΩ, another negative pressure was given to rupture the cell membrane and cell-attached current clamp was performed. The data acquisition and analysis were performed online with pClamp10.

2.9. *Viral injection, optical fiber implantation and fiber photometry recording*

To detect the real-time cAMP changes in the MSNs, we ordered a recombinant adeno-associated virus of cAMP probe that specifically express Pink Flamindo[45,46], rAAV2/9-EF1α-DIO-Pink Flamindo-WPRE-hGH polyA (BrainVTA). For bilateral stereotaxic injection, D1-Cre or D2-Cre mice were anesthetized with isoflurane and fixed in the stereotaxic instrument (RWD Life Science). The coordinates of NAc were as follows: anteroposterior +1.6 mm, mediolateral ±1.3 mm, and dorsoventral −4.4 mm, according to the bregma. A microinjection pump was used to infuse 0.5 μL virus (rAAV2/9-EF1α-DIO-Pink Flamindo-WPRE-hGH polyA, $\geq 5 \times 10^{12}$ v.g./mL) at a rate of 0.1 μL/min. The needle was retained for 10 min before removal. All virus-injected mice were post-experimentally verified for virus injection placement according to the expression of Pink Flamindo; mice with an incorrect placement or no detectable expression were excluded from the experimental groups.

For fiber photometry recording experiment, an optical fiber (4.5 mm in length, 1.5 mm outer diameter) was placed in the NAc on the same day of virus injection. Mice were paired housed to recover for 2 weeks. The real-time fluorescence signals of cAMP were acquired using the three-color single-channel optical fiber recording system (Thinker Tech Fiber Photometry). Behavioral events or drug treatments were marked in each trial. The photometry data were exported to MATLAB for further analysis. The values of fluorescence change ($\Delta F/F$) were calculated by $(F-F_0)/F_0$, and the F_0 refers to the baseline fluorescence before

the stimulation events within each trial. The changing curves of cAMP in D1 or D2 MSNs were presented with average plots or heatmaps.

2.10. Stereotaxic surgery and viral gene transfer

To respectively reduce endogenic cAMP in D1-MSNs, D2-MSNs, or simultaneously both in D1-MSNs and D2-MSNs, we customized the Cre-dependent AAV virus of shRNA-Adcy5. For D1-MSNs cAMP knockdown, the mixed viruses AAV2/9-D1-Cre-WPRE-hGH pA and AAV2/9-CAG-DIO-EGFP-shRNA-Adcy5-WPREs, titer ratio, 1:3, were stereotactically injected into bilateral NAc as previously described. For D2-MSNs cAMP knockdown, the mixed viruses AAV2/9-D2-Cre-WPRE-hGH pA and AAV2/9-CAG-DIO-EGFP-shRNA-Adcy5-WPREs, titer ratio, 1:3, were stereotactically injected into bilateral NAc. For both D1-MSNs and D2-MSNs cAMP knockdown, the mixed viruses AAV2/9-D1-Cre-WPRE-hGH pA, AAV2/9-D2-Cre-WPRE-hGH pA and AAV2/9-CAG-DIO-EGFP-shRNA-Adcy5-WPREs, titer ratio, 1:1:3, were stereotactically injected into bilateral NAc. The control virus used AAV2/9-shRNA(scramble). All of the viruses were ordered from Shumi (Wuhan, China). All mice were *post hoc* screened according to the expression of EGFP.

2.11. Chemogenetics for activation or inhibition

AAV2/9-DIO-Gi, AAV2/9-DIO-Gs or AAV2/9-DIO-Gq was respectively mixed with AAV2/9-D1-Cre or AAV2/9-D2-Cre, titer ratio, 3:1. Mice were anesthetized with isoflurane and fixed well in the small-animal stereotaxic instrument, a volume of 0.5 μL mixed viruses was bilaterally infused into the NAc (AP, +1.6 mm and ML, ±1.3 mm from the bregma; DV, −4.4 mm from the brain surface) using micro-injection pump at a rate of 0.1 μL/min. The needle was retained for 10 min to minimize spread of the virus along the injection track[15,17]. Mice were housed to express DREADDs for 2 weeks, and were injected with 1 mg/kg CNO for inhibition or activation. All mice were *post hoc* screened according to the expression of EGFP.

2.12. ELISA analysis

The levels of cAMP in plasma and tissue homogenate were measured using the Direct cAMP ELISA Kit (NewEast Bioscience). To examine the liver and kidney damage, H&E stained liver and kidney sections were routinely assessed for the morphology and inflammatory lesion. For biochemical indexes determination, liver and kidney homogenates were made in PBS, and the supernatant was collected to measure alanine aminotransferase (ALT), aspartate aminotransferase (AST), alkaline phosphatase (ALP), urea nitrogen (BUN), creatinine (CRE), uric acid (UA), using commercially-available kits (Nanjing Jiancheng, China).

2.13. Statistical analysis

All behavioral experiments were analyzed by investigators blinded to the treatment. Mice were randomly grouped and the sample sizes are indicated by dots in the figures or are stated in the figure legends. All data are presented as the mean ± standard error of mean (SEM), and the values that were greater than 2 SD from the mean were identified as outliers and excluded from further statistics. Statistical analyses were performed using GraphPad Prism 7.0, ImageJ, pClamp10 or MATLAB. After normality and equal variance tests, the differences were evaluated using one-way or two-way ANOVA (followed by Bonferroni's *post hoc* comparisons and $P < 0.05$ was defined as statistically significant). Social interaction tests were analyzed using ANY-maze (Stoelting, USA).

3. Results

3.1. Social stress vulnerability is associated with reduced cAMP in a subset of D1-MSNs in the NAc

The chronic social defeat stress (CSDS) paradigm is well established to induce a depression-like phenotype in a subset of mice, termed stress-susceptible (SS) mice, while the others are stress resilient (RES) mice (Fig. 1A–C). We consistently found down-regulation of cAMP in the NAc of SS mice but not RES mice (Fig. 1D). Given that 95% of neurons in the NAc are dopamine D1 receptor medium spiny neurons (D1-MSNs) and dopamine D2 receptor medium spiny neurons (D2-MSNs), which is different from the conventional opinion that D1-MSNs mediate reward effects and D2-MSNs encode aversion effects, cumulative studies have revealed that both D1-MSNs and D2-MSNs could orchestrate reward and aversion. To further elucidate the subtle change in cAMP levels in D1-MSNs and D2-MSNs of SS mice, we crossed the D1-Cre or D2-Cre mouse line with a Cre-dependent tdTomato reporter line to visualize D1-MSNs or D2-MSNs (Supporting Information Fig. S1A). We found a substantial population of tdTomato-positive neurons in the striatum of D1-tdTomato and D2-tdTomato mice, indicating a high expression efficiency in the mouse strains we created (Fig. S1B). We next employed in situ hybridization to verify the accuracy of these tdTomato-labeled neurons. The RNAscope fluorescent staining results showed that 95.73% of tdTomato-positive neurons were coexpressed with D1 mRNA in the D1-tdTomato mouse strain, whereas only a small fraction of D2 mRNA was tdTomato positive (Fig. S1C). Similarly, 94.58% of tdTomato-positive neurons were coexpressed with D2 mRNA in the D2-tdTomato mouse strain (Fig. S1D). These results indicate good expression accuracy of tdTomato. We also confirmed the functionality of these tdTomato-labeled neurons. Electrophysiological recordings showed that D1-tdTomato-positive neurons exhibited a lower frequency relative to D1-tdTomato-negative neurons, indicating the electrophysiological characteristics of D1-MSNs (Fig. S1E and S1F). For D2-tdTomato mice, the higher frequency of D2-tdTomato-positive neurons also exhibited the electrophysiological characteristics of D2-MSNs (Fig. S1G and S1H). Together, these results demonstrate that these mouse strains are reliable. We next performed immuno-colocalization analyses to determine whether the decrease in cAMP levels in the NAc of SS mice occurred in D1-MSNs or D2-MSNs, using D1-tdTomato and D2-tdTomato mice. Immunostaining revealed that cAMP was markedly decreased in the NAc of SS mice, and precisely reduced within D1-tdTomato-positive MSNs, but not D1-tdTomato-negative MSNs (Fig. 1E and F). Consistently, D2-tdTomato SS mice showed distinctly lower cAMP in D2-tdTomato-negative MSNs (Fig. 1G and H).

cAMP is a second messenger synthesized within the cell and orchestrates numerous physiological responses including regulating transcription factors, ion channels, excitability, and synaptic plasticity[24,47–51]. We assumed that cAMP levels were dynamically altered along with different stimulations and emotional

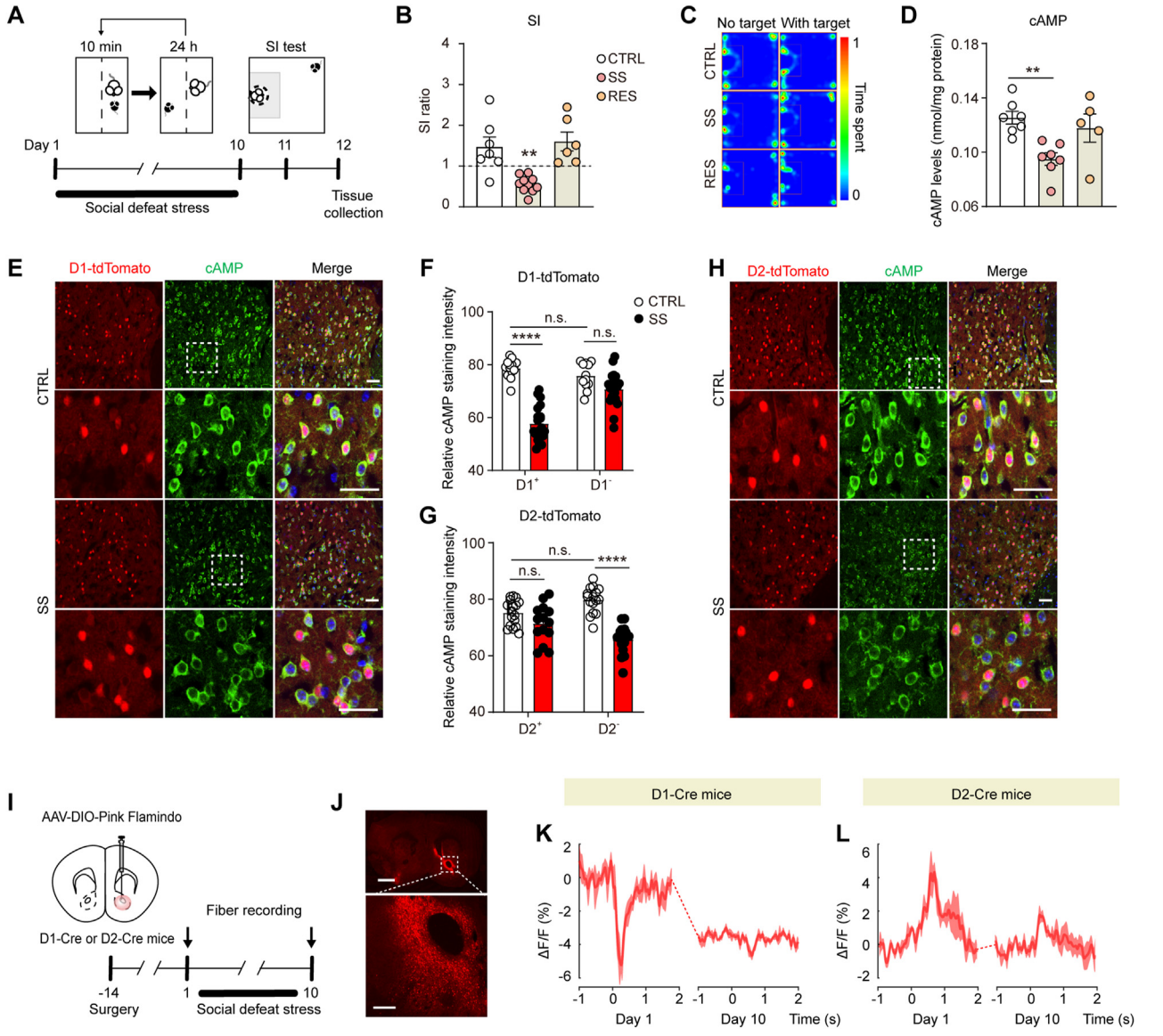

Figure 1 Cyclic adenosine monophosphate (cAMP) in the dopamine D1 receptor medium spiny neurons (D1-MSNs) of nucleus accumbens (NAc) is reduced in depressed mice. (A) Schematic representation of the chronic social defeat stress (CSDS) procedure. (B) The social interaction (SI) ratio, stressed mice were divided into susceptible (SS) and resilient (RES) phenotypes, one-way ANOVA followed by Bonferroni's multiple comparison test, $F_{(2,\ 20)} = 12.1$, $P = 0.0004$. (C) Heat maps visualizing the time spent in the SI test. (D) cAMP levels (measured by ELISA) in the NAc of depressed mice, one-way ANOVA followed by Bonferroni's multiple comparison test, $F_{(2,\ 16)} = 6.957$, $P = 0.0067$. (E) cAMP staining and co-labeled with D1-tdTomato in the NAc, scale bars, 20 μm. Staining intensity was quantified (F, G), two-way ANOVA followed by Bonferroni's multiple comparison test, $F_{(1,\ 64)} = 85.24$, $P < 0.0001$ in (F), $F_{(1,\ 58)} = 14.51$, $P = 0.0003$ in (G). (H) cAMP staining and co-labeled with D2-tdTomato in the NAc, scale bars, 20 μm. (I) Schematic representation of viral injection and fiber recording. (J) Representation of the expression of Pink Flamindo in the whole brain (left), scale bars, 1 mm, the right is a representation showing of the expression of Pink Flamindo in the NAc, scale bars, 100 μm. (K) The plots of group average cAMP responses to the onset of social defeat stress on 1 day and 10 days in D1-cre mice, the same F_0 was intercepted from the 1st day, $n = 5$ mice. (L) The plots of group average cAMP responses to the onset of social defeat stress on 1 day and 10 days in D2-cre mice, the same F_0 was intercepted from the 1st day, $n = 5$ mice. The number of experimental subjects is indicated by the dots in the figures. Data represent mean ± SEM, $^{**}P < 0.01$, $^{****}P < 0.0001$, n.s., no significance. CTRL, control; SS, stress susceptible; SI, social interaction.

valences. Herein, we constructed a cAMP fluorescence probe to interrogate the adaptive changes in cAMP in D1-MSNs and D2-MSNs of the NAc (Fig. 1I and Supporting Information Fig. S2A). We confirmed the substantial expression of the Pink Flamindo probe in the NAc (Fig. 1J). To understand how cAMP responds to stimuli, we employed four natural reward and aversive stimuli. Consequently, the photometry recording showed that there was no cAMP signal response to sucrose licking, sniffing a female stranger and tail suspension (Fig. S2B and S2C). The onset of social defeat stress triggered a marked decrease in the cAMP signal in D1-MSNs but an increase in the cAMP signal in D2-MSNs, indicating that only intense stimuli, such as defeat stress, were sufficient to induce changes in cAMP in the NAc (Fig. S2B and S2C). To further demonstrate the dynamic changes in

cAMP in D1-MSNs and D2-MSNs of the NAc during the 10-day CSDS paradigm, we examined the cAMP response before and after the social defeat period. The photometry recording showed that the marked decline in cAMP in D1-MSNs induced by social defeat was dampened after the CSDS paradigm, and the baseline level of cAMP in D1-MSNs was also reduced (Fig. 1K). In contrast, we found that social defeat stress caused an unremarkable increase in cAMP in D2-MSNs (Fig. 1L). Together, these findings indicate that the SS mice are associated with reduced cAMP in a subset of D1-MSNs in the NAc.

3.2. *cAMP in the subset of D1-MSNs in the NAc mediates social stress vulnerability*

To confirm the causal role of cAMP in NAc D1-MSNs in social stress-induced depression-like behaviors, we conducted conditional knockdown of adenylate cyclase 5 (*Adcy5*, cAMP synthetase, which is predominantly expressed in the NAc among the 10 subtypes[17]) in D1-MSNs, D2-MSNs or both D1-and D2-MSNs to modulate the neuronal cAMP concentration in the NAc *in vivo* (Fig. 2A and Supporting Information Fig. S3A). We confirmed

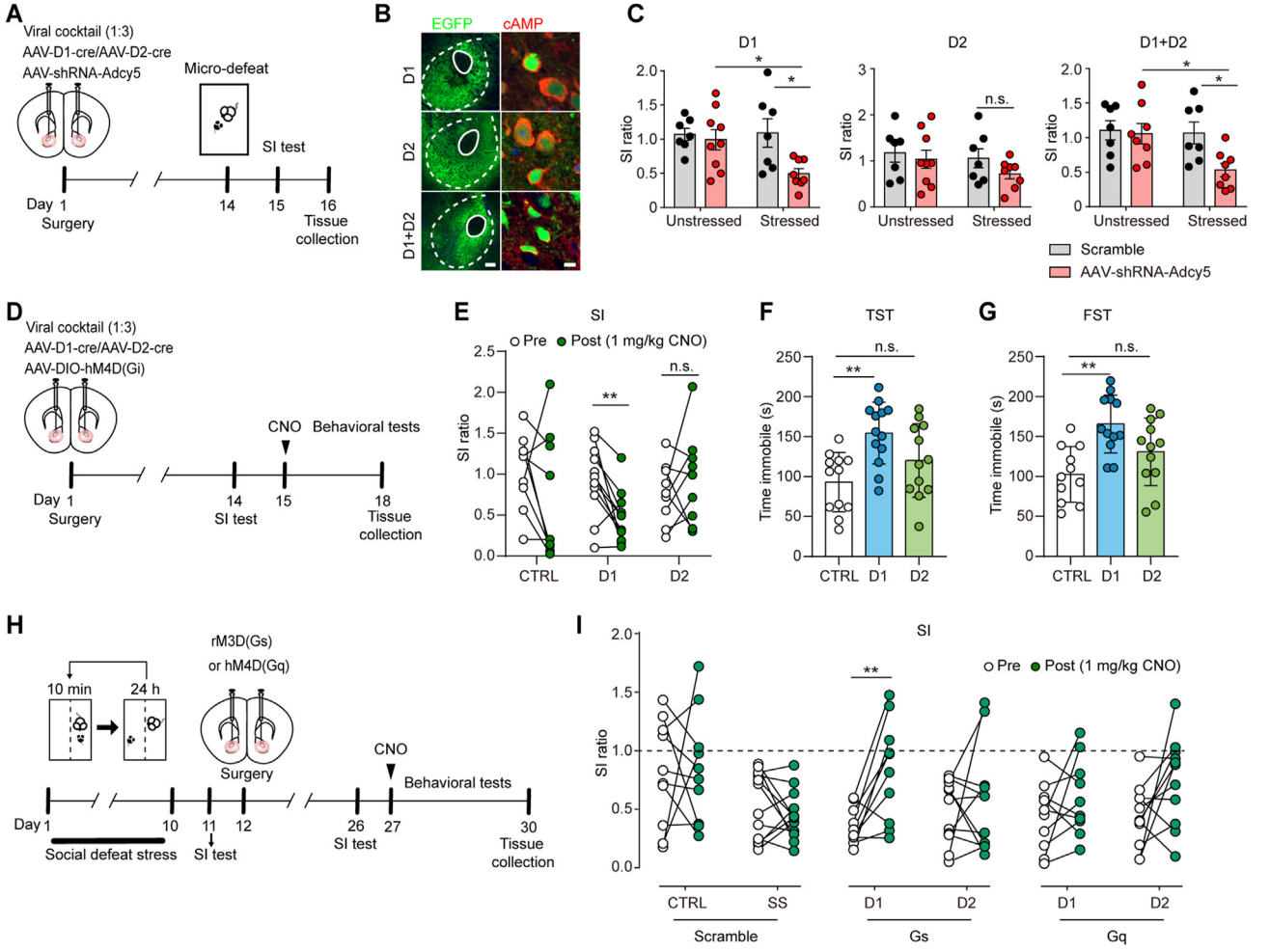

Figure 2 cAMP in NAc D1-MSNs mediates social stress vulnerability. (A) Schematic showing the experimental design of viral injection and micro-defeat stress paradigm, Mixed D1 represents AAV2/9-D1-Cre-WPRE-hGH pA and AAV2/9-CAG-DIO-EGFP-shRNA-Adcy5-WPREs, titer ratio, 1:3; Mixed D2 represents AAV2/9-D2-Cre-WPRE-hGH pA and AAV2/9-CAG-DIO-EGFP-shRNA-Adcy5-WPREs, titer ratio, 1:3; Mixed D1+D2 represents AAV2/9-D1-Cre-WPRE-hGH pA, AAV2/9-D2-Cre-WPRE-hGH pA and AAV2/9-CAG-DIO-EGFP-shRNA-Adcy5-WPREs, titer ratio, 1:1:3. The control group used instead of AAV2/9-CAG-DIO-EGFP-shRNA(scramble)-WPREs. (B) The representative fluorescent images showing the expression of EGFP in the NAc (left) and the level of cAMP in the NAc (right), scale bars (left, 100 μm; right, 10 μm). (C) Individual social interaction ratio values on Day 15. Two-way ANOVA followed by Bonferroni's multiple comparison test, $F_{(1,\ 27)} = 3.434$, $P = 0.0748$ of D1, $F_{(1,\ 27)} = 0.2897$, $P = 0.5948$ of D2, $F_{(1,\ 26)} = 3.165$, $P = 0.0869$ of D1+D2. (D) Schematic showing the experimental design of AAV-Gi injection. (E) Individual SI ratio values before and after CNO injection. Paired *t*-test, $t = 1.272$, d.f. $= 8$, $P = 0.2391$ of CTRL, $t = 3.638$, d.f. $= 10$, $P = 0.0045$ of D1, $t = 0.8466$, d.f. $= 8$, $P = 0.4218$ of D2. Quantification of the immobile time in the TST (F) and FST (G), one-way ANOVA followed by Bonferroni's multiple comparison test, $F_{(2,\ 34)} = 7.145$, $P = 0.0026$ in (F), $F_{(2,\ 32)} = 7.963$, $P = 0.0016$ in (G). (H) Schematic showing the experimental design of social defeat stress and AAV injection. (I) Individual SI ratio values in each group, paired *t*-test, $t = 3.634$, d.f. $= 9$, $P = 0.0055$ of D1-Gs, $t = 0.6243$, d.f. $= 10$, $P = 0.5464$ of D2-Gs. The number of experimental subjects is indicated by the dots in the figures. Data represent mean ± SEM, $^*P < 0.05$, $^{**}P < 0.01$, n.s., no significance. CTRL, control; SI, social interaction; TST, tail suspension test; FST, forced swimming test.

viral expression in the NAc, and immunofluorescence co-localization analysis revealed the downregulation of cAMP (Fig. 2B and Fig. S3B). After 2 weeks of recovery, the mice were subjected to a subthreshold micro-defeat to investigate the susceptibility to depression. As a result, a reduction in cAMP levels in D1-MSNs combined with subthreshold micro-defeat was sufficient to induce social avoidance behavior, but a reduction in cAMP levels in D2-MSNs was not (Fig. 2C). Moreover, the simultaneous cAMP reduction in D1-and D2-MSNs in combination with exposure to subthreshold micro-defeat also markedly induced social avoidance behavior (Fig. 2C). These results consistently suggest that cAMP in NAc D1-MSNs plays a vital role in stress susceptibility. We next used the hM4D(Gi) inhibitory DREADD (designer receptors exclusively activated by designer drugs) construct to inhibit the production of cAMP in the presence of clozapine-*N*-oxide (CNO) (Fig. 2D and Fig. S3C). Inhibition of NAc D2-MSNs had no effect on depression-like behaviors (Fig. 2E−G). However, intraperitoneal administration of CNO (1 mg/kg) to inhibit NAc D1-MSNs induced a significant decline in the SI ratio (social avoidance behavior, Fig. 2E), and markedly increased immobility time in the TST and FST (Fig. 2F and G). Stereotaxic intra-NAc infusion of a D1R antagonist (SCH23390) also significantly reduced the SI ratio and increased the immobility time in the TST (Fig. S3D and S3E), and no difference was observed with D2R antagonist (eticlopride) infusion.

To further examine the effect of cAMP in NAc D1-MSNs on depression-like behaviors, another cohort of mice was conducted rM3D(Gs) or hM3D(Gq) DREADD to activate D1-MSNs or D2-MSNs (Fig. 2H and Fig. S3C). rM3D(Gs) is particularly used to induce the production of cAMP and hM3D(Gq) activation is widely used to induce intracellular calcium release in the presence of CNO. Unexpectedly, only chemogenetic activation of D1-MSNs by rM3D(Gs) notably improved depression-like behaviors, wherein the mice displayed a higher SI ratio (Fig. 2I), spent less immobile time in the TST and FST, and reversed anhedonia as assessed by the sucrose preference test (Fig. S3F−S3H). In contrast, chemogenetic activation of D2-MSNs had no effect on depression-like behaviors. Furthermore, no difference was observed in mice that had received hM3D(Gq) activation in either D1-MSNs or D2-MSNs (Fig. 2I and Fig. S3F−S3H). Furthermore, stereotaxic intra-NAc infusion of a D1R agonist (SKF81297) but not a D2R agonist (quinpirole) reversed social avoidance (Fig. S3I) and significantly reduced the immobility time in the TST (Fig. S3I and S3J). These results suggest that cAMP reduction in NAc D1-MSNs promoted stress susceptibility, and the stimulation of cAMP production in NAc D1-MSNs could reverse depression-like behaviors.

3.3. The rapid antidepressant effect of ketamine depends on elevating cAMP in D1-MSNs in the NAc

Considering that ketamine was arguably discovered to elicit fast and sustained antidepressant effects by a single administration, we next evaluated the effect of a single ketamine injection on cAMP signaling in depressed mice. We first elucidated the effect of ketamine treatment on cAMP in depressed mice by immunocolocalization analyses using D1-tdTomato and D2-tdTomato mice (Fig. 3A). After a 10-day CSDS paradigm, only the SS mice were selected to receive administration of ketamine or vehicle (Fig. 3A and Supporting Information Fig. S4A). As shown in Fig. 3B, cAMP levels in D1-tdTomato-positive MSNs were notably reduced in SS mice, and a single ketamine administration was sufficient to improve cAMP levels in D1-tdTomato-positive MSNs. In addition, there was no significant difference in cAMP levels in D2-tdTomato-positive MSNs of SS mice, but ketamine markedly elevated cAMP in D2-tdTomato-positive MSNs (Fig. 3C and D). We next performed intra-NAc injection of AAV-DIO-Pink Flamindo into D1-Cre or D2-cre mice (Fig. S4B), and after a 10-day CSDS paradigm, the mice were divided into the SS and RES groups according to the SI ratio (Fig. S4C). The onset of social defeat triggered a decrease in the cAMP signal in D1-MSNs and an increase in the cAMP signal in D2-MSNs of SS mice; however, a single administration of ketamine enhanced cAMP in both D1-MSNs and D2-MSNs (Fig. S4D).

To further determine whether the increased cAMP level in D1-MSNs or D2-MSNs mediated the antidepressant effect of a single administration of ketamine, we next knocked down *Adcy5* to decrease the level of cAMP in D1-MSNs or D2-MSNs *in vivo* (Fig. 3E). The mixed viruses of AAV-D1-Cre or AAV-D2-Cre with Cre-dependent adeno-associated virus targeting shRNA transcripts encoding *Adcy5* allowed for reduced synthesis of endogenous cAMP, which was confirmed by the downregulation of cAMP through immunofluorescence (Fig. S4D). We next investigated the impact of reductive cAMP on the antidepressant effect of ketamine, and consistently found that the reduction in cAMP in D1-MSNs counteracted the effects of ketamine to relieve depression. In the SI test and TST, ketamine treatment notably improved the SI ratio and lessened the immobility time in the shRNA-scramble group and D2 knockdown group; however, reducing cAMP in D1-MSNs in combination with ketamine treatment had no effect on the behaviors, as well as reducing cAMP both in D1 and D2-MSNs in combination with ketamine (Fig. 3F and G). In the FST, ketamine treatment was effective in ameliorating the desperate behavior in the shRNA-scramble group, but no obvious effect was observed in the knockdown groups (Fig. 3H). The anhedonic behavior tested by the SPT was recovered in all of the mice at the time of the test (Fig. S4F). Another cohort of mice that underwent hM4D(Gi) inhibition was also used to evaluate which cAMP signal mediated the antidepressant effect of ketamine treatment (Fig. 3J). Injection of scramble viruses did not affect the antidepressant effect of ketamine, however, D1-MSN inhibition by hM4D(Gi) eliminated the effect of ketamine (Fig. 3I, K, L).

Altogether, these data suggest that ketamine treatment enhanced cAMP both in D1-MSNs and D2-MSNs of SS mice, but only the increased cAMP level in D1-MSNs mediated the antidepressant effect of ketamine.

3.4. Crocin elevates cAMP in the NAc and rapidly relieves depression within 24 h

It is plausible that elevating cAMP in the NAc, especially D1-MSNs, could promote the development of effective antidepressant drugs. With this in mind, psychoactive drugs were screened, and we found that higher dose of crocin (the main hydrosoluble active ingredient of saffron) could markedly increase cAMP levels in the NAc of SS mice (Fig. 4A, Supporting Information Fig. S5A and Table S1). Next, we employed the chronic unpredictable mild stress (CUMS) model to study the antidepressant effect of crocin (Fig. 4B). It was amazing to find that 300 mg/kg of crocin administration markedly improved anhedonia (sucrose preference) (Fig. 4C) and grooming (coat score) (Fig. 4D) in one week, while citalopram and low-dose of crocin took effect only after four weeks of treatment (Fig. 4C and D).

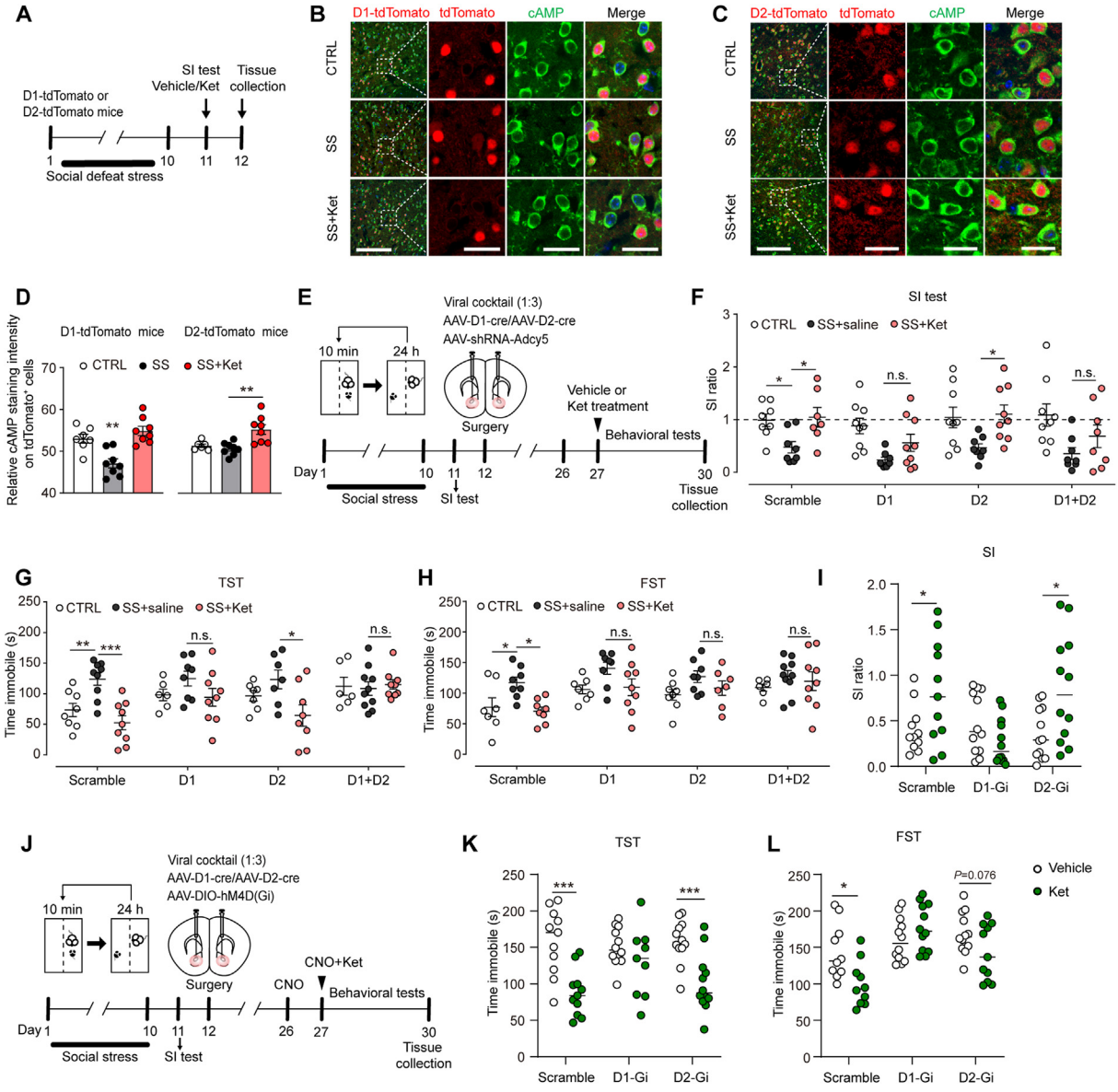

Figure 3 D1-MSNs cAMP mediate the rapid antidepression effect of a single acute ketamine injection. (A) Schematic representation of social defeat stress paradigm and immunofluorescence of cAMP in D1-tdTomato mice and D2-tdTomato mice. (B) Representative images of cAMP staining and co-labeled with D1-tdTomato in the NAc. scale bars (left), 100 μm, and scale bars of the enlarged images (right), 20 μm. (C) Representative images of cAMP staining and co-labeled with D2-tdTomato in the NAc. scale bars (left), 100 μm, and scale bars of the enlarged images (right), 20 μm. (D) Statistic of cAMP staining intensity on tdTomato$^+$ MSNs after ketamine injection in D1-tdTomato mice (top) and D2-tdTomato mice (bottom). The dots represent the number of neurons from 4 different regions of 3 mice. One-way ANOVA followed by Bonferroni's multiple comparison test, $F_{(2,\ 20)} = 14.43$, $P = 0.0001$ of D1-tdTomato mice and $F_{(2,\ 19)} = 9.533$, $P = 0.0014$ of D2-tdTomato mice. (E) Schematic showing the experimental design of defeat stress paradigm and viral injection. (F) SI ratio values on Day 28. One-way ANOVA followed by Bonferroni's multiple comparison test, $F_{(2,\ 20)} = 5.284$, $P = 0.0144$ of shRNA-scramble, $F_{(2,\ 23)} = 5.626$, $P = 0.0103$ of D1, $F_{(2,23)} = 4.553$, $P = 0.0216$ of D2, $F_{(2,\ 22)} = 3.864$, $P = 0.0365$ of D1+D2. The immobile time in the TST on Day 29 (G) and FST on Day 30 (H). One-way ANOVA followed by Bonferroni's multiple comparison test, (G) $F_{(2,\ 23)} = 11.86$, $P = 0.0003$ of shRNA-scramble, $F_{(2,\ 20)} = 1.7$, $P = 0.2080$ of D1, $F_{(2,19)} = 4.141$, $P = 0.0322$ of D2, $F_{(2,\ 22)} = 0.1064$, $P = 0.8995$ of D1+D2; (H) $F_{(2,\ 20)} = 5.962$, $P = 0.0093$ of shRNA-scramble, $F_{(2,\ 21)} = 2.82$, $P = 0.0823$ of D1, $F_{(2,20)} = 2.344$, $P = 0.1217$ of D2, $F_{(2,\ 23)} = 0.9566$, $P = 0.3990$ of D1+D2. (I) Individual SI ratio values, unpaired *t*-test with equal variance, $t = 2.156$, d.f. $= 20$, $P = 0.0435$ of scramble, $t = 1.66$, d.f. $= 22$, $P = 0.1112$ of D1-Gi, $t = 2.605$, d.f. $= 22$, $P = 0.0162$ of D2-Gi. (J) Schematic showing the experimental design of defeat stress paradigm and viral injection. (K) Quantification of the immobile time in the TST, unpaired *t*-test with equal variance, $t = 4.287$, d.f. $= 20$, $P = 0.0004$ of scramble, $t = 1.3$, d.f. $= 19$, $P = 0.2091$ of D1-Gi, $t = 4.038$, d.f. $= 22$, $P = 0.0006$ of D2-Gi. (L) Quantification of the immobile time in the FST, unpaired *t*-test with equal variance, $t = 2.863$, d.f. $= 18$, $P = 0.0103$ of scramble, $t = 1.313$, d.f. $= 22$, $P = 0.2027$ of D1-Gi, $t = 1.866$, d.f. $= 21$, $P = 0.0761$ of D2-Gi. The number of experimental subjects is indicated by the dots in the figures. Data represent mean ± SEM, $^*P < 0.05$, $^{**}P < 0.01$, $^{***}P < 0.001$, n.s., no significance. SI, social interaction; CTRL, control; SS, stress susceptible; TST, tail suspension test; FST, forced swimming test; Ket, ketamine.

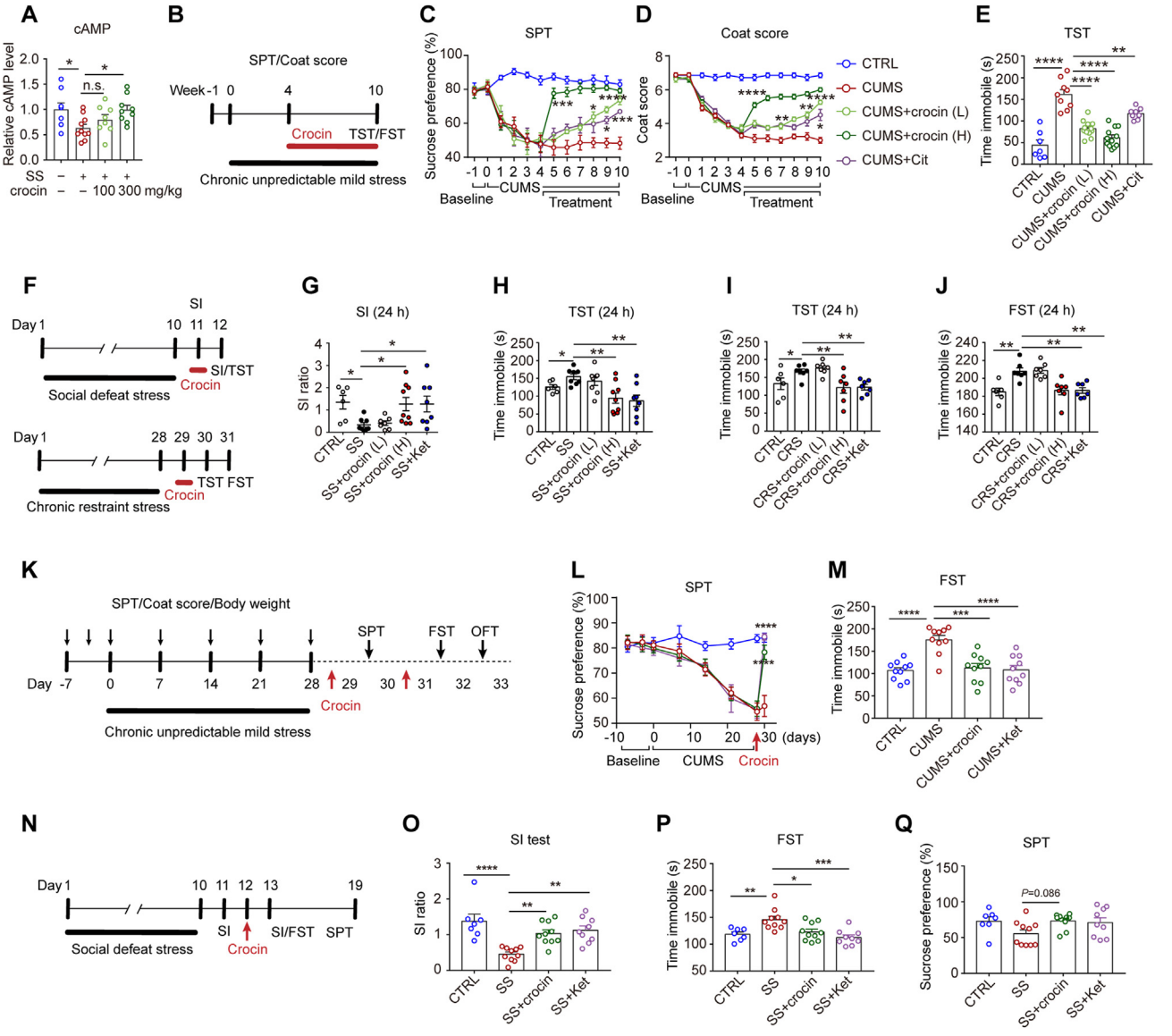

Figure 4 Crocin elevates cAMP in the NAc and rapidly relieves depression within 24 h. (A) cAMP levels in the NAc, one-way ANOVA followed by Bonferroni's multiple comparison test, $F_{(3,\ 31)} = 3.725$, $P = 0.0214$. (B) Schematic representation of the chronic unpredictable mild stress (CUMS) procedure and drug treatment. Crocin (L:100 mg/kg or H: 300 mg/kg) was intragastrically (i.g.) administered and citalopram (20 mg/kg) was intraperitoneally (i.p.) administered, once daily. Measurements of sucrose preference (C) and coat score (D) at each week, mixed effects analysis, $F_{(44,\ 428)} = 5.16$, $P < 0.0001$ in (C); $F_{(44,\ 473)} = 15.92$, $P < 0.0001$ in (D). (E) Quantification of the immobile time in the TST, one-way ANOVA followed by Bonferroni's multiple comparison test, $F_{(4,\ 43)} = 32.23$, $P < 0.0001$. (F) Schematic representation of the chronic social defeat stress (CSDS) procedure, chronic restraint stress (CRS) procedure and drug treatments. crocin (300 mg/kg) was i.g. administered, ketamine (10 mg/kg) was i.p. administered. (G, H) Behavioral tests of SI and TST, one-way ANOVA followed by Bonferroni's multiple comparison test, $F_{(4,\ 31)} = 3.752$, $P = 0.0133$ in (G); $F_{(4,\ 34)} = 5.736$, $P = 0.0012$ in (H). (I, J) Behavioral tests of TST and FST, one-way ANOVA followed by Bonferroni's multiple comparison test, $F_{(4,\ 27)} = 7.158$, $P = 0.0005$ in (I); $F_{(4,\ 29)} = 10.22$, $P < 0.0001$ in (J). (K) Schematic representation of the chronic unpredictable mild stress (CUMS) procedure and drug treatment. Crocin (300 mg/kg, i.g.) and ketamine (10 mg/kg, i.p.) were administered and behavioral tests were performed 24 h later. (L) Measurements of sucrose preference at each week or after drug administration, mixed effects analysis, $F_{(21,\ 288)} = 5.876$, $P < 0.0001$. (M) The immobile time in the FST, one-way ANOVA followed by Bonferroni's multiple comparison test, $F_{(3,\ 36)} = 13.23$, $P < 0.0001$. (N) Schematic representation of the chronic social defeat stress (CSDS) procedure and drug treatment (crocin, 300 mg/kg, i.g., and ketamine, 10 mg/kg, i.p.). (O) SI ratio values, one-way ANOVA followed by Bonferroni's multiple comparison test, $F_{(3,\ 32)} = 11.08$, $P < 0.0001$. The immobile time in the FST (P) and SPT (Q), one-way ANOVA followed by Bonferroni's multiple comparison test, $F_{(3,\ 32)} = 7.789$, $P = 0.0005$ in (P); $F_{(3,\ 32)} = 2.644$, $P = 0.0660$ in (Q). The number of experimental subjects is indicated by the dots in the figures or illustrated in the legends. Data represent mean ± SEM, $^{*}P < 0.05$, $^{**}P < 0.01$, $^{***}P < 0.001$, $^{****}P < 0.0001$. CTRL, control mice; SS, stress susceptible; Cit, citalopram; Ket, ketamine; SI, social interaction; TST, tail suspension test; FST, forced swimming test; SPT, sucrose preference test; CUMS, chronic unpredictable mild stress; CRS, chronic restraint stress.

This was consistent with the result that high-dose of crocin markedly increased cAMP levels in the NAc, but not lower dose. Moreover, both crocin and citalopram administration significantly decreased the total duration of immobility in the TST (Fig. 4E) and FST (Fig. S5B) after 6 weeks of treatment, suggesting that high-dose of crocin rapidly relieved depression while lower dose crocin took effect slowly like citalopram. This finding could also be confirmed by the recorded instances that accidently taken massive saffron would cause over-stimulated[52]. It should be noted that the SPT and coat score were assessed once a week, and one week of high-dose crocin treatment completely rescued the depression-like behaviors. To further examine the rapid antidepressant effects of crocin, we employed the CSDS paradigm, and behavioral tests were performed at 2 and 24 h after crocin administration (Fig. 4F). Crocin was less able to improve social avoidance behavior 2 h after administration (Fig. S5C and S5D) but ketamine was effective in reducing the immobility time in the TST (Fig. S5D). Notably, 24 h later, both ketamine and high-dose of crocin stably rescued depression-like behaviors, including social avoidance and behavioral despair (as measured by the immobility time in the TST and FST) (Fig. 4G, H, and Fig. S5E). Our collaborators employed another animal model of depression, mice with chronic restraint stress (CRS), and confirmed that high-dose crocin treatment markedly rescued depression-like behaviors 24 h after administration (Fig. 4I, J, and Fig. S5F).

Importantly, the rapid antidepressant effect of high-dose crocin that relieves depression 24 h later was also verified by independent and single-blind experimenters in another institution using CUMS and CSDS paradigms. After four weeks of CUMS, the depressed mice were intragastrically administered crocin (300 mg/kg) or intraperitoneally injected with ketamine (Fig. 4K). As a result, both crocin and ketamine treatments notably improved sucrose preference (Fig. 4L) and markedly decreased the total duration of immobility in the FST (Fig. 4M). No effect was observed in the open field test (OFT) (Fig. S5G). Another cohort of mice that underwent CSDS was also reversed by crocin treatment (Fig. 4N) and displayed a markedly increased SI ratio (Fig. 4O) and reduced immobility time in the FST (Fig. 4P). SPT was performed several days later and the anhedonia of most SS mice had recovered by that time (Fig. 4Q).

Given that only high-dose of crocin was effective to rapidly relieve depression (a high dose of 300 mg/kg partly because the molecular weight of crocin is 976.97), we next initially examined the system safety of 300 mg/kg crocin. After the continuous administration for one week, the indices of liver (ALT, AST, ALP) and those of kidney (BUN, CRE, UA) showed no difference relative to the control mice (Supporting Information Fig. S6A−S6F). Histologic staining showed no tissue damage and inflammation (Fig. S6G). Moreover, no neurotoxicity was observed by behavioral assessments (Fig. S6H−S6Q). These experiments indicated that the doses of crocin used in these experiments were safe.

Together, these studies from independent animal facilities by different experimenters strongly suggested the great potential and advantage of high-dose crocin in rapidly relieving depression.

3.5. Elevating cAMP in D1-MSNs in the NAc is necessary for the antidepressant effect of crocin

Given that 300 mg/kg crocin elevates cAMP in the NAc and rapidly relieves depression, we next evaluated the particular neuron type of crocin modulation. First, using D1-tdTomato and D2-tdTomato mice, the immune-colocalization analyses consistently revealed that the cAMP level was notably reduced in D1-MSNs of SS mice, and crocin treatment markedly improved cAMP levels in D1-MSNs (Fig. 5A−C). Unlike ketamine, crocin treatment had no effect on cAMP levels in D2-MSNs (Fig. 5C). We next employed the cre-dependent AAV-shRNA-Adcy5 virus to reduce the synthesis of endogenous cAMP in D1-MSNs or D2-MSNs *in vivo* (Fig. 5D). Viral expression and the down-regulation of cAMP were confirmed by immunofluorescence (Supporting Information Fig. S7A). In the shRNA-scramble group, crocin treatment notably improved the SI ratio (Fig. 5E) and decreased the immobility time in the FST (Fig. 5F) and TST (Fig. 5G). However, the reduction in cAMP in D1-MSNs counteracted the effects of crocin to rapidly relieve depression (Fig. 5E−G). Moreover, we consistently found that the anhedonic behavior of the SS mice had recovered two weeks after the CSDS paradigm and no difference was observed in the SPT (Fig. S7B). A reduction in cAMP levels in D2-MSNs had no effect on the antidepressant effect of crocin (Fig. S7C). However, in another cohort of mice, endogenous cAMP was reduced in both D1-MSNs and D2-MSNs, crocin treatment was less able to ameliorate depression-like behaviors (Fig. S7D).

To further elucidate the necessity of elevating cAMP in D1-MSNs for the antidepressant effect of crocin, we also employed an hM4D(Gi)-inhibitory DREADD construct to inhibit the production of cAMP in D1-MSNs or D2-MSNs (Fig. 5H and Fig. S7E). One cohort of mice treated with AAV-scramble showed that CNO injection did not affect the antidepressant effect of crocin (Fig. 5I−K). However, D1-MSN inhibition by hM4D(Gi) eliminated the effects of crocin on improving social avoidance (Fig. 5I) and behavioral despair (Fig. 5J and K). Another cohort of mice that underwent hM4D(Gi) inhibition in D2-MSNs was still improved by crocin treatment (Fig. 5I−K). Altogether, these data suggest that elevating cAMP in D1-MSNs in the NAc is necessary for the antidepressant effect of crocin.

4. Discussion

Overall, our results suggest that improving cAMP levels in D1-MSNs of the NAc is a potential therapeutic strategy for rapid antidepressant treatment and provide a candidate drug, crocin, that rapidly relieves depression by regulating D1-MSN cAMP signaling in the NAc. These findings facilitate the development of new rapid antidepressants.

Accumulating evidence suggests the crucial role of cAMP in depression, especially the cAMP levels in the NAc, as enhancing cAMP levels in the NAc could rescue depressive symptoms[17,23,24,53,54]. Ketamine has also been reported to relieve depression by increasing cAMP levels rather than targeting NMDA receptors[22]. In addition, cAMP signaling in the NAc may act as an emotional response, triggered by both programing reward valuation and the actions of addictive drugs[55−62]. Acute opioid exposure can cause rewarding effects and enhance cAMP signaling in D1-MSNs, while prolonged opioid exposure has been linked to aversive phenotypes and suppressing D1-MSN cAMP signaling but enhancing D2-MSN signaling[55]. Our studies suggested that D1-MSN cAMP was notably reduced in SS mice, and there was no obvious change of D2-MSN cAMP. However, it is notable that ketamine treatment simultaneously increased cAMP levels in D1-MSNs and D2-MSNs, which may mediate the antidepressant effects as well as the side effects of ketamine. In contrast, crocin treatment specifically increased cAMP in NAc D1-MSNs which may be connected with less side effects of

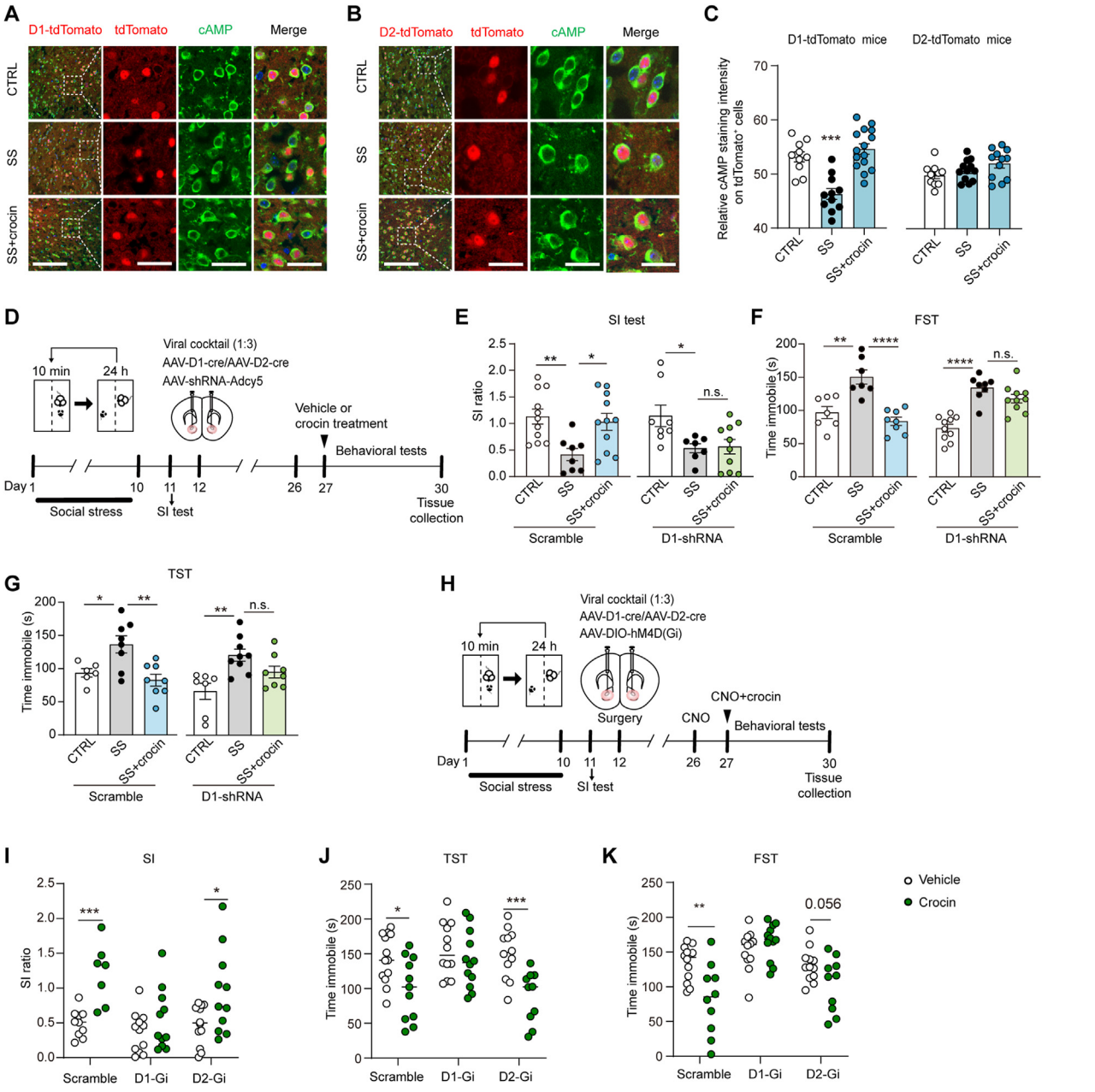

Figure 5 Elevating cAMP in D1-MSNs in the NAc is necessary for the antidepressant effect of crocin. (A) Representative images of cAMP staining and co-labeled with D1-tdTomato in the NAc, scale bars (left), 100 μm, and scale bars of the enlarged images (right), 20 μm. (B) Representative images of cAMP staining and co-labeled with D2-tdTomato in the NAc. scale bars (left), 100 μm, and scale bars of the enlarged images (right), 20 μm. (C) Statistic of cAMP staining intensity on tdTomato^{+} MSNs in D1-tdTomato mice (top) and D2-tdTomato mice (bottom). The dots represent the number of neurons from 4 different regions of 3 mice. One-way ANOVA followed by Bonferroni's multiple comparison test, $F_{(2,\ 33)} = 20.57$, $P < 0.0001$ of D1-tdTomato mice and $F_{(2,\ 31)} = 4.898$, $P = 0.0142$ of D2-tdTomato mice. (D) Schematic showing the experimental design of defeat stress paradigm and viral injection. (E) SI ratio values on Day 28. One-way ANOVA followed by Bonferroni's multiple comparison test, $F_{(2,\ 27)} = 6.233$, $P = 0.0060$ of scramble, $F_{(2,\ 22)} = 4.901$, $P = 0.0174$ of D1-shRNA. (F) The immobile time in the FST on Day 29. One-way ANOVA followed by Bonferroni's multiple comparison test, $F_{(2,\ 19)} = 16.56$, $P < 0.0001$ of scramble, $F_{(2,\ 24)} = 27.69$, $P < 0.0001$ of D1-shRNA. (G) The immobile time in the TST on Day 30. One-way ANOVA followed by Bonferroni's multiple comparison test, $F_{(2,\ 19)} = 8.132$, $P = 0.0028$ of scramble, $F_{(2,\ 21)} = 7.491$, $P = 0.0035$ of D1-shRNA. (H) Schematic showing the experimental design of defeat stress paradigm and viral injection. (I) SI ratio values, unpaired *t*-test with equal variance, $t = 4.576$, d.f. $= 15$, $P = 0.0004$ of scramble, $t = 1.16$, d.f. $= 21$, $P = 0.2593$ of D1-Gi, $t = 2.343$, d.f. $= 21$, $P = 0.0290$ of D2-Gi. (J) The immobile time in the TST, unpaired *t*-test with equal variance, $t = 2.676$, d.f. $= 22$, $P = 0.0138$ of scramble, $t = 0.878$, d.f. $= 22$, $P = 0.3894$ of D1-Gi, $t = 3.953$, d.f. $= 20$, $P = 0.0008$ of D2-Gi. (K) The immobile time in the FST, unpaired *t*-test with equal variance, $t = 3.086$, d.f. $= 20$, $P = 0.0058$ of scramble, $t = 1.082$, d.f. $= 22$, $P = 0.2909$ of D1-Gi, $t = 2.029$, d.f. $= 20$, $P = 0.0560$ of D2-Gi. The number of experimental subjects is indicated by the dots in the figures. Data represent mean ± SEM, $^{*}P < 0.05$, $^{**}P < 0.01$, $^{***}P < 0.001$, $^{****}P < 0.0001$, n.s., no significance. SI, social interaction; CTRL, control; SS, stress susceptible; TST, tail suspension test; FST, forced swimming test.

crocin. To our knowledge, this is the first study to provide a candidate drug, crocin, to regulate D1-MSN cAMP signaling in the NAc, in addition to addictive drugs. Our study shows that crocin has potential application value as a psychoactive antidepressant.

Another advantage of this study is that we first highlighted a higher dose of crocin as a psychoactive drug to rapidly and robustly relieve depression within 24 h after a single oral administration, while lower dose of crocin might gradually take effect over weeks. The pharmacological doses adopted in most preclinical studies for crocin were 20−200 mg/kg[39,63,64], and crocin was reported to elicit antidepressant effect after continuously given for at least 4 weeks[64−67]. Our findings complement previous evidence suggesting that a higher dose of crocin can rapidly relieve depression. Moreover, our pilot experiments suggest that crocin was superior at relieving depression at doses greater than 200 mg/kg by intragastric administration in mice. It seems plausible because the psychoactive substances always act varying at different doses. More importantly, crocin is quite safe and possibly has fewer psychotomimetic side effects and abuse liability, which requires more peer verification. What is currently known is that crocin should not be used on patients with hemorrhagic spots because of its ability to invigorate the circulation of blood and remove blood stasis[68−71].

Our findings demonstrate the crucial role of D1-MSN cAMP in depression; however, the role of D2-MSN cAMP has not been elucidated. Further work is required to illuminate the specific behavior that is involved in D2-MSN cAMP regulation. Given that D1-MSNs and D2-MSNs receive different projections and form neural circuits, respectively, their involvement in the regulation of cAMP production is multifaceted. Extensive experiments are needed to elucidate the specific neural circuits involved in D1-MSNs to D2-MSNs and to achieve precise neural circuit regulation. A greater understanding of the targeted regulation of endogenous cAMP could promote the development of effective antidepressant drugs.

Together, we show here that improving D1-MSN cAMP can rapidly reverse the depressive behaviors, opening a new avenue for developing therapeutics for depression. We also provide crocin as a drug candidate.

5. Conclusions

We identified a specific reduction of cAMP in the subset of D1-MSNs in the NAc that promoted stress susceptibility. Crocin efficiently stimulated the production of cAMP in NAc D1-MSNs thus rescued depression-like behaviors, showing outstanding potential for clinical translation.

Acknowledgments

This study was supported by National Natural Science Foundation of China (No. 82104278), Leading Technology Foundation Research Project of Jiangsu Province (No. BK20192005, China), National Key Project of Science and Technology for Innovation Drugs of China (No. 2017ZX09301013), CAMS Innovation Fund for Medical Sciences (CIFMS, No. 2021-I2M-5-011, China), Sanming Project of Medicine in Shenzhen (No. SZSM201801060, China), Project of State Key Laboratory of Natural Medicines, China Pharmaceutical University (No. SKLNMKF202203, China), National Innovation and Entrepreneurship Training Program for Undergraduate, China Pharmaceutical University (Nos. 202310316138 1 and 202310316128 7, China). The authors would like to thank the sharing platform for the use of large-scale experimental apparatuses at the State Key Laboratory of National Medicines, China Pharmaceutical University.

Author contributions

Yue Zhang, Hao Hong, Peng Xu, Yuan Xie, Tianming Gao, Youmei Wang and Xiaotian Li: conceptualization, methodology, writing-original draft and writing-reviewing and editing. Yue Zhang, Jingwen Gao, Na Li, Jinqian Cheng, Mingrui Wang, Xueru Li, Shimeng Qu, Yaheng Song, Fan Xiao, Ronghao Mu, Xinyu Yang, and Jihong Liu: methodology and investigation. Na Li, Ronghao Mu, Xinyu Yang, Jihong Liu and Fan Xiao: methodology and resources. Yue Zhang, Jiye Aa, Guangji Wang: conceptualization, supervision, writing-reviewing and editing and funding acquisition.

Conflicts of interest

The authors declare no conflict of interest.

Appendix A. Supporting information

Supporting data to this article can be found online at https://doi.org/10.1016/j.apsb.2023.12.005.

References

1. Tang F, Liang J, Zhang H, Kelifa MM, He QQ, Wang PG. COVID-19 related depression and anxiety among quarantined respondents. *Psychol Health* 2021;**36**:164−78.
2. Rabeea SA, Merchant HA, Khan MU, Kow CS, Hasan SS. Surging trends in prescriptions and costs of antidepressants in England amid COVID-19. *Daru* 2021;**29**:217−21.
3. Sun H, Damez-Werno DM, Scobie KN, Shao NY, Dias C, Rabkin J, et al. ACF chromatin-remodeling complex mediates stress-induced depressive-like behavior. *Nat Med* 2015;**21**:1146−53.
4. Wang J, Hodes GE, Zhang H, Zhang S, Zhao W, Golden SA, et al. Epigenetic modulation of inflammation and synaptic plasticity promotes resilience against stress in mice. *Nat Commun* 2018;**9**:477.
5. Sullivan PF, Neale MC, Kendler KS. Genetic epidemiology of major depression: review and meta-analysis. *Am J Psychiatry* 2000;**157**:1552−62.
6. Zhang ZW, Gao CS, Zhang H, Yang J, Wang YP, Pan LB, et al. *Morinda officinalis* oligosaccharides increase serotonin in the brain and ameliorate depression *via* promoting 5-hydroxytryptophan production in the gut microbiota. *Acta Pharm Sin B* 2022;**12**:3298−312.
7. Zhang L, Hu K, Shao T, Hou L, Zhang S, Ye W, et al. Recent developments on PET radiotracers for TSPO and their applications in neuroimaging. *Acta Pharm Sin B* 2021;**11**:373−93.
8. Bagot RC, Parise EM, Pena CJ, Zhang HX, Maze I, Chaudhury D, et al. Ventral hippocampal afferents to the nucleus accumbens regulate susceptibility to depression. *Nat Commun* 2015;**6**:7062.
9. Hu H. Reward and aversion. *Annu Rev Neurosci* 2016;**39**:297−324.
10. Lammel S, Lim BK, Ran C, Huang KW, Betley MJ, Tye KM, et al. Input-specific control of reward and aversion in the ventral tegmental area. *Nature* 2012;**491**:212−7.
11. Watabe-Uchida M, Zhu L, Ogawa SK, Vamanrao A, Uchida N. Whole-brain mapping of direct inputs to midbrain dopamine neurons. *Neuron* 2012;**74**:858−73.
12. Bekhbat M, Li Z, Mehta ND, Treadway MT, Lucido MJ, Woolwine BJ, et al. Functional connectivity in reward circuitry and symptoms of anhedonia as therapeutic targets in depression with high

inflammation: evidence from a dopamine challenge study. *Mol Psychiatr* 2022;**27**:4113−21.
13. LeGates TA, Kvarta MD, Tooley JR, Francis TC, Lobo MK, Creed MC, et al. Reward behaviour is regulated by the strength of hippocampus-nucleus accumbens synapses. *Nature* 2018;**564**:258−62.
14. Willmore L, Cameron C, Yang J, Witten IB, Falkner AL. Behavioural and dopaminergic signatures of resilience. *Nature* 2022;**611**:124−32.
15. Menard C, Pfau ML, Hodes GE, Kana V, Wang VX, Bouchard S, et al. Social stress induces neurovascular pathology promoting depression. *Nat Neurosci* 2017;**20**:1752−60.
16. Krishnan V, Han MH, Graham DL, Berton O, Renthal W, Russo SJ, et al. Molecular adaptations underlying susceptibility and resistance to social defeat in brain reward regions. *Cell* 2007;**131**:391−404.
17. Zhang Y, Lu W, Wang Z, Zhang R, Xie Y, Guo S, et al. Reduced neuronal cAMP in the nucleus accumbens damages blood−brain barrier integrity and promotes stress vulnerability. *Biol Psychiatr* 2020;**87**:526−37.
18. Chen G, Lai S, Bao G, Ke J, Meng X, Lu S, et al. Distinct reward processing by subregions of the nucleus accumbens. *Cell Rep* 2023;**42**:112069.
19. Al-Hasani R, McCall JG, Shin G, Gomez AM, Schmitz GP, Bernardi JM, et al. Distinct subpopulations of nucleus accumbens dynorphin neurons drive aversion and reward. *Neuron* 2015;**87**:1063−77.
20. Liu Z, Le Q, Lv Y, Chen X, Cui J, Zhou Y, et al. A distinct D1-MSN subpopulation down-regulates dopamine to promote negative emotional state. *Cell Res* 2022;**32**:139−56.
21. Chen R, Blosser TR, Djekidel MN, Hao J, Bhattacherjee A, Chen W, et al. Decoding molecular and cellular heterogeneity of mouse nucleus accumbens. *Nat Neurosci* 2021;**24**:1757−71.
22. Wray NH, Schappi JM, Singh H, Senese NB, Rasenick MM. NMDAR-independent, cAMP-dependent antidepressant actions of ketamine. *Mol Psychiatr* 2019;**24**:1833−43.
23. Fujita M, Richards EM, Niciu MJ, Ionescu DF, Zoghbi SS, Hong J, et al. cAMP signaling in brain is decreased in unmedicated depressed patients and increased by treatment with a selective serotonin reuptake inhibitor. *Mol Psychiatr* 2017;**22**:754−9.
24. Plattner F, Hayashi K, Hernandez A, Benavides DR, Tassin TC, Tan C, et al. The role of ventral striatal cAMP signaling in stress-induced behaviors. *Nat Neurosci* 2015;**18**:1094−100.
25. O'Donnell JM, Xu Y. Evidence for global reduction in brain cyclic adenosine monophosphate signaling in depression. *Biol Psychiatr* 2012;**72**:524−5.
26. Reiach JS, Li PP, Warsh JJ, Kish SJ, Young LT. Reduced adenylyl cyclase immunolabeling and activity in postmortem temporal cortex of depressed suicide victims. *J Affect Disord* 1999;**56**:141−51.
27. Garcia AM, Martinez A, Gil C. Enhancing cAMP levels as strategy for the treatment of neuropsychiatric disorders. *Curr Top Med Chem* 2016;**16**:3527−35.
28. Monleon S, D'Aquila P, Parra A, Simon VM, Brain PF, Willner P. Attenuation of sucrose consumption in mice by chronic mild stress and its restoration by imipramine. *Psychopharmacology (Berl)* 1995;**117**:453−7.
29. Golden SA, Covington 3rd HE, Berton O, Russo SJ. A standardized protocol for repeated social defeat stress in mice. *Nat Protoc* 2011;**6**:1183−91.
30. Kim KS, Han PL. Optimization of chronic stress paradigms using anxiety- and depression-like behavioral parameters. *J Neurosci Res* 2006;**83**:497−507.
31. Yu Z, Kong D, Liang Y, Zhao X, Du G. Protective effects of VMY-2-95 on corticosterone-induced injuries in mice and cellular models. *Acta Pharm Sin B* 2021;**11**:1903−13.
32. Slattery DA, Cryan JF. Using the rat forced swim test to assess antidepressant-like activity in rodents. *Nat Protoc* 2012;**7**:1009−14.
33. Liu MY, Yin CY, Zhu LJ, Zhu XH, Xu C, Luo CX, et al. Sucrose preference test for measurement of stress-induced anhedonia in mice. *Nat Protoc* 2018;**13**:1686−98.
34. Alonso R, Griebel G, Pavone G, Stemmelin J, Le Fur G, Soubrie P. Blockade of CRF_1 or V_{1b} receptors reverses stress-induced suppression of neurogenesis in a mouse model of depression. *Mol Psychiatr* 2004;**9**:278−86,224.
35. Surget A, Saxe M, Leman S, Ibarguen-Vargas Y, Chalon S, Griebel G, et al. Drug-dependent requirement of hippocampal neurogenesis in a model of depression and of antidepressant reversal. *Biol Psychiatr* 2008;**64**:293−301.
36. Li XY, Han Y, Zhang W, Wang SR, Wei YC, Li SS, et al. AGRP neurons project to the medial preoptic area and modulate maternal nest-building. *J Neurosci* 2019;**39**:456−71.
37. Zhang L, Koller J, Ip CK, Gopalasingam G, Bajaj N, Lee NJ, et al. Lack of neuropeptide FF signalling in mice leads to reduced repetitive behavior, altered drinking behavior, and fuel type selection. *FASEB J* 2021;**35**:e21980.
38. Siracusa R, Paterniti I, Cordaro M, Crupi R, Bruschetta G, Campolo M, et al. Neuroprotective effects of temsirolimus in animal models of Parkinson's disease. *Mol Neurobiol* 2018;**55**:2403−19.
39. Zhang Y, Fei F, Zhen L, Zhu X, Wang J, Li S, et al. Sensitive analysis and simultaneous assessment of pharmacokinetic properties of crocin and crocetin after oral administration in rats. *J Chromatogr B Anal Technol Biomed Life Sci* 2017;**1044−1045**:1−7.
40. Zhang Y, Geng JL, Hong Y, Jiao L, Li SN, Sun RB, et al. Orally administered crocin protects against cerebral ischemia/reperfusion injury through the metabolic transformation of crocetin by gut microbiota. *Front Pharmacol* 2019;**10**:440.
41. Jung ES, Lee HJ, Sim HR, Baik JH. Cocaine-induced behavioral sensitization in mice: effects of microinjection of dopamine d2 receptor antagonist into the nucleus accumbens. *Exp Neurobiol* 2013;**22**:224−31.
42. Huang CS, Wang GH, Chuang HH, Chuang AY, Yeh JY, Lai YC, et al. Conveyance of cortical pacing for parkinsonian tremor-like hyperkinetic behavior by subthalamic dysrhythmia. *Cell Rep* 2021;**35**:109007.
43. Guilherme EM, Gianlorenco ACL. The effects of intravermis cerebellar microinjections of dopaminergic agents in motor learning and aversive memory acquisition in mice. *Front Behav Neurosci* 2021;**15**:628357.
44. Shen CJ, Zheng D, Li KX, Yang JM, Pan HQ, Yu XD, et al. Cannabinoid CB1 receptors in the amygdalar cholecystokinin glutamatergic afferents to nucleus accumbens modulate depressive-like behavior. *Nat Med* 2019;**25**:337−49.
45. Harada K, Ito M, Wang X, Tanaka M, Wongso D, Konno A, et al. Red fluorescent protein-based cAMP indicator applicable to optogenetics and *in vivo* imaging. *Sci Rep* 2017;**7**:7351.
46. Stierl M, Stumpf P, Udwari D, Gueta R, Hagedorn R, Losi A, et al. Light modulation of cellular cAMP by a small bacterial photoactivated adenylyl cyclase, bPAC, of the soil bacterium *Beggiatoa*. *J Biol Chem* 2011;**286**:1181−8.
47. Atkins CM, Oliva Jr AA, Alonso OF, Pearse DD, Bramlett HM, Dietrich WD. Modulation of the cAMP signaling pathway after traumatic brain injury. *Exp Neurol* 2007;**208**:145−58.
48. Batty NJ, Fenrich KK, Fouad K. The role of cAMP and its downstream targets in neurite growth in the adult nervous system. *Neurosci Lett* 2017;**652**:56−63.
49. Cerny O, Anderson KE, Stephens LR, Hawkins PT, Sebo P. cAMP signaling of adenylate cyclase toxin blocks the oxidative burst of neutrophils through Epac-mediated inhibition of phospholipase C activity. *J Immunol* 2017;**198**:1285−96.
50. Dwivedi Y, Pandey GN. Adenylyl cyclase-cyclicAMP signaling in mood disorders: role of the crucial phosphorylating enzyme protein kinase A. *Neuropsychiatric Dis Treat* 2008;**4**:161−76.
51. Ren X, Mody I. gamma-Hydroxybutyrate induces cyclic AMP-responsive element-binding protein phosphorylation in mouse hippocampus: an involvement of $GABA_B$ receptors and cAMP-dependent protein kinase activation. *Neuroscience* 2006;**141**:269−75.

52. Baker D, Negbi K. Uses of saffron. *Econ Bot* 1983;**37**:228−36.
53. Chen X, Luo J, Leng Y, Yang Y, Zweifel LS, Palmiter RD, et al. Ablation of type III adenylyl cyclase in mice causes reduced neuronal activity, altered sleep pattern, and depression-like phenotypes. *Biol Psychiatr* 2016;**80**:836−48.
54. Rasenick MM. Depression and adenylyl cyclase: sorting out the signals. *Biol Psychiatr* 2016;**80**:812−4.
55. Muntean BS, Dao MT, Martemyanov KA. Allostatic changes in the cAMP system drive opioid-induced adaptation in striatal dopamine signaling. *Cell Rep* 2019;**29**:946−60.e2.
56. Soares-Cunha C, de Vasconcelos NAP, Coimbra B, Domingues AV, Silva JM, Loureiro-Campos E, et al. Nucleus accumbens medium spiny neurons subtypes signal both reward and aversion. *Mol Psychiatr* 2020;**25**:3241−55.
57. Sutton LP, Muntean BS, Ostrovskaya O, Zucca S, Dao M, Orlandi C, et al. NF1−cAMP signaling dissociates cell type-specific contributions of striatal medium spiny neurons to reward valuation and motor control. *PLoS Biol* 2019;**17**:e3000477.
58. Muntean BS, Zucca S, MacMullen CM, Dao MT, Johnston C, Iwamoto H, et al. Interrogating the spatiotemporal landscape of neuromodulatory GPCR signaling by real-time imaging of cAMP in intact neurons and circuits. *Cell Rep* 2018;**22**:255−68.
59. Lobo MK, Nestler EJ. The striatal balancing act in drug addiction: distinct roles of direct and indirect pathway medium spiny neurons. *Front Neuroanat* 2011;**5**:41.
60. Di Chiara G, Imperato A. Drugs abused by humans preferentially increase synaptic dopamine concentrations in the mesolimbic system of freely moving rats. *Proc Natl Acad Sci U S A* 1988;**85**:5274−8.
61. Self DW, Barnhart WJ, Lehman DA, Nestler EJ. Opposite modulation of cocaine-seeking behavior by D1- and D2-like dopamine receptor agonists. *Science* 1996;**271**:1586−9.
62. Volkow ND, Fowler JS, Wang GJ, Baler R, Telang F. Imaging dopamine's role in drug abuse and addiction. *Neuropharmacology* 2009;**56**(Suppl 1):3−8.
63. Naghizadeh B, Mansouri MT, Ghorbanzadeh B, Farbood Y, Sarkaki A. Protective effects of oral crocin against intracerebroventricular streptozotocin-induced spatial memory deficit and oxidative stress in rats. *Phytomedicine* 2013;**20**:537−42.
64. Xiao Q, Shu R, Wu C, Tong Y, Xiong Z, Zhou J, et al. Crocin-I alleviates the depression-like behaviors probably *via* modulating "microbiota−gut−brain" axis in mice exposed to chronic restraint stress. *J Affect Disord* 2020;**276**:476−86.
65. Wu R, Tao W, Zhang H, Xue W, Zou Z, Wu H, et al. Instant and persistent antidepressant response of Gardenia yellow pigment is associated with acute protein synthesis and delayed upregulation of BDNF expression in the hippocampus. *ACS Chem Neurosci* 2016;**7**:1068−76.
66. Talaei A, Hassanpour Moghadam M, Sajadi Tabassi SA, Mohajeri SA. Crocin, the main active saffron constituent, as an adjunctive treatment in major depressive disorder: a randomized, double-blind, placebo-controlled, pilot clinical trial. *J Affect Disord* 2015;**174**:51−6.
67. Amin B, Nakhsaz A, Hosseinzadeh H. Evaluation of the antidepressant-like effects of acute and sub-acute administration of crocin and crocetin in mice. *Avicenna J Phytomed* 2015;**5**:458−68.
68. Zhang Y, Guo C, Liu H, Yang L, Ren C, Li T, et al. Multiplex quantitation of 17 drug-derived components in human plasma after administration of a fixed herbal preparation of Sailuotong using combined online SPE-LC−MS/MS methods. *J Ethnopharmacol* 2023;**302**:115843.
69. Ma XQ, Zhu DY, Li SP, Dong TT, Tsim KW. Authentic identification of stigma Croci (stigma of *Crocus sativus*) from its adulterants by molecular genetic analysis. *Planta Med* 2001;**67**:183−6.
70. Xing B, Li S, Yang J, Lin D, Feng Y, Lu J, et al. Phytochemistry, pharmacology, and potential clinical applications of saffron: a review. *J Ethnopharmacol* 2021;**281**:114555.
71. Feng P, Li Q, Liu L, Wang S, Wu Z, Tao Y, et al. Crocetin prolongs recovery period of DSS-induced colitis *via* altering intestinal microbiome and increasing intestinal permeability. *Int J Mol Sci* 2022;**23**:3832.